Solvent-Free and TMEDA-Solvated Mixed Alkali Metal-Magnesium Tris-diisopropylamides

Eva Hevia,[a] Fiona R. Kenley,[a] Alan R. Kennedy,[a] Robert E. Mulvey,*[a] and René B. Rowlings[a]

Dedicated to the memory of Ron Snaith

Keywords: Alkali metals / N ligands / Heterometallic complexes / Potassium / Magnesium

A trio of heterobimetallic tris-diisopropylamides, the solvent-free potassium-magnesium amide [$\{KMg(N\mathit{i}Pr_2)_3\}_\infty$], its TMEDA solvate [$KMg(N\mathit{i}Pr_2)_3$·TMEDA] and the sodium congener [$NaMg(N\mathit{i}Pr_2)_3$·TMEDA] has been synthesised by mixing the appropriate metal alkyl reagents with three molar equivalents of diisopropylamine in a hydrocarbon medium, to which, in the last two cases, TMEDA is added. All three amides have been successfully crystallographically characterised by X-ray diffraction studies. Representing the first pure *s*-block mixed-metal diisopropylamide free of solvent molecules or other stabilising anionic co-ligands, the first compound adopts an infinite spiral chain of ···K-(μ-N)$_2$-Mg-N··· links, the metal-N framework of which is supported by agostic K···C intra-dinuclear and inter-dinuclear contacts. The dinuclear tris-amido motif is maintained in both TMEDA complexes, the metal-N cores of which are essentially isostructural, but the presence of the chelating diamine blocks the propagating terminal site on the alkali metal and so gives rise to discrete molecular structures.

Introduction

Generally dispensed in the form of its lithium compound, the sterically demanding diisopropylamido ligand ($\mathit{i}Pr_2N^-$, DA; with lithium, LDA) has long commanded a high-ranking position in synthesis on account of its good (kinetic) basicity and poor nucleophilicity. These complementary properties combine to make LDA the shelf reagent of choice in a legion of proton abstraction applications (especially with weakly acidic organic compounds).[1] When planning a synthesis it would be a tactical error to view LDA as simply a convenient source of DA, as the presence of the lithium counterion imparts (or affects) certain characteristics of the amide [including, for example, aggregation state/s; extent and nature of solvation; polarity and strength of the metal-N bond; hybridisation of the anionic N centre; solubility; thermal stability; susceptibility to β-hydride elimination from the $Me_2C(H)$- branches], which can have a profound effect on the outcome and rate of a reaction with a substrate.[2] Though patterns can be discerned and rationalised in certain systems, in general metal effects in metal-mediated reactions can be a minefield of complexity, which can only be safely trodden through by assessing the influence of each metal on an individual basis.[3] It follows that changing the metal supporting the DA ligand from lithium to another metal can bring about significant differences in the reactivity/selectivity and kinetics of the amido functionality. This is one reason for synthesising new metal complexes of DA. We have an additional incentive for pursuing such a goal. The DA ligand has played a major role in advancing our work in *s*-block metal synergy and "inverse crown" chemistry. So called because of their inverse topological relationship to conventional crown ether complexes, inverse crowns are poly-mixed-metal amide cationic ring compounds with anionic centres.[4] DA has served as the metal atom linking unit in inverse crowns with alkoxo [$\{MMg(DA)_2OR\}_2$] (M = Li, R = *n*Oct; M = Na, R = *n*Bu or *n*Oct),[5] hydrido [$Na_2Mg_2(DA)_4(H)_2$·(toluene)$_2$][6] or ferrocenetetrayl [$Na_4Mg_4(DA)_8\{Fe(C_5H_3)_2\}$] cores,[7] where it performs a μ_2 bonding role. The "super" inverse crown structure of [$\{NaMg(DA)(O)$·$(THF)\}_6$][8] also has μ_2-DA ligands in the sodium amide appendages to the hexameric $(MgO)_6$ cage. Common to the synthesis of each of these species is a synergic tris-amide of general formula [$MMg(DA)_3$], though hitherto no structural information has been available on these inverse crown precursors. Here we report the first isolated and crystallographically characterised such tris-diisopropylamides in the solvent-free, mixed potassium-magnesium polymer [$\{KMg(DA)_3\}_\infty$] **1**, its diamine-solvated analogue [$KMg(DA)_3$·TMEDA] **2**, and for comparison the mixed sodium-magnesium solvate [$NaMg(DA)_3$·TMEDA] **3** [where TMEDA = *N*,*N*,*N*′,*N*′-tetramethylethylenediamine,

---

[a] Department of Pure and Applied Chemistry, University of Strathclyde,
Glasgow, G1 1XL, U.K.

DOI: 10.1002/ejic.200300413

$Me_2N(CH_2)_2NMe_2$]. A survey of the literature also reveals that the significance of **1** goes beyond its relevance to inverse crown chemistry as, to the best of our knowledge, it represents the first pure *s*-block heterobimetallic diisopropylamide, pure in the sense that it is free of stabilising anionic co-ligands or neutral solvent ligands. Such a pure form is also unknown in homometallic systems if one discounts the crystal structure of LDA itself, as this was determined from a sample which contained small, non-stoichiometric quantities of TMEDA and the parent amine DAH.

Results and Discussion

The new compounds **1−3** were prepared by the same mixed-metallation strategy [Equation (1)]: metal alkyl reagents are stirred together in a hydrocarbon medium, before the introduction of the required quantity of DAH to convert all of the alkyl substituents to gaseous alkane (or to an arene in the case of the benzyl substituents), leaving the desired heterobimetallic amide mixture in solution. The preparation of **1** from *n*-butylpotassium is not straightforward. While crystals of **1** can be grown reproducibly in low yields, they are invariably accompanied by variable amounts of an oily residue and a black waxy solid, the characterisation of which was not pursued. This decomposition is almost certainly triggered by β-hydride elimination from *n*-butylpotassium in the main (prior to the alkane generation stage) and possibly from DA ligands — it has been reported previously that homometallic $Mg(DA)_2$ suffers a thermally induced hydride elimination from one of its β-C atoms, in a process which can be subsequently exploited to reduce aldehydes or ketones to alcohols.[9] Heating the reaction solution of **1** above ambient temperature proves particularly detrimental, leading to more black waxy solid residue. Switching to benzylpotassium seems to produce a cleaner reaction, though the yield of **1**, whilst better, does not improve vastly. When toluene is added as a co-solvent the reaction solution can even tolerate reflux conditions using this resonance-stabilised reagent, however, under such conditions the reaction follows a different course, generating hydride ions, which ultimately end up in the new inverse crown species $[K_2Mg_2(DA)_4(H)_2\cdot(toluene)_2]$, as discussed in the following paper in this issue.[10] To complete the formation of both **2** and **3**, TMEDA is added in an additional step. While in comparison to that for **1** it is a more routine task to crystallise these TMEDA complexes (by cooling the resulting solutions to −28 °C) it is not easy to collect all of the crystalline product/s by vacuum filtration. This is because the crystals of both **2** and **3** readily dissolve in hexane/heptane solution at ambient temperature, hence the isolation procedure is best carried out at subambient temperature (even then, a large proportion of the crystalline material is visibly lost). Such exceptionally good solubility in hydrocarbon media pointed to a synergic effect with both metal atoms intimately involved in the crystalline structures (as confirmed later by the X-ray crystallographic studies, vide infra), as on their own NaDA/KDA exhibit little or no solubility in hexane/heptane and their solvated offspring $[(NaDA\cdot TMEDA)_2]$[11] and $[(KDA\cdot TMEDA)_2]$[12] only limited solubility. The solubilising effect of mixing alkali metal and magnesium compounds in certain systems has also been noted in alkoxide chemistry.[13] As expected, the synergic influence has no bearing on the air instability of **1−3** as all are highly sensitive to moisture and oxygen.

$$RM + Bu_2Mg + 3iPr_2NH \rightarrow \text{“}MMg(NPri_2)_3\text{”} + 2BuH + RH \quad (1)$$

Solvent-free **1** dissolves in arene solvents allowing a ^1H NMR spectrum to be recorded in [D$_6$]benzene solution. At room temperature a single type of amide *i*Pr group [$(CH_3)_2CH$ septet at δ = 3.38 ppm; $(CH_3)_2CH$ doublet at δ = 1.27 ppm] is revealed. This is consistent with either chemically distinct amide ligands undergoing a fast exchange process or chemically equivalent ligands. With respect to the crystal structure, the former scenario could involve the exchanging of bridging and terminal groups within a “$K(\mu\text{-}DA)_2MgDA$” molecule, while the latter scenario could be envisioned as a discrete $[Mg(DA)_3]^-$ “ate” with the K^+ counterion sequestered by π-binding arene solvent ligands (alkali metal π-arene interactions, which have been observed in several inverse crown complexes, are believed to be of fundamental structural importance to a wide range of materials).[14,15] In both these scenarios the agostic $K\cdots C(H)(CH_3)_2/K\cdots C(H_3)C(H)(CH_3)$ intermolecular interactions extending the molecular structure in the solid state would be absent in solution. The corresponding spectrum of **3** also reveals a single type of amido *i*Pr group, but the chemical shifts of the $CH(CH_3)_2$ septet (δ =3.50 ppm) and the $CH(CH_3)_2$ doublet (δ =1.38 ppm) show a modest yet significant move to higher frequency compared to those in **1** (by 0.12 and 0.11 ppm respectively) suggesting that a $[Mg(DA)_3]^-$ “ate” anion is not common to both species. These chemical shifts in **3** also differ from those in homometallic $[(NaDA\cdot TMEDA)_2]$[11] (corresponding values δ = 3.66 and 1.26 ppm) where the DA ligand bridging is exclusively to Na^+ centres. In $[(NaDA\cdot TMEDA)_2]$ it was reasoned that TMEDA is not bound to the Na^+ centres in [D$_6$]benzene solution at room temperature on account of the relative positioning of the TMEDA resonances [CH_2CH_2N at δ = 2.13 ppm; $(CH_3)_2N$ at δ = 2.08 ppm]; when TMEDA is ligated to the metal the situation is reversed. Significantly, the latter case, and at notably lower chemical shift values [$(CH_3)_2N$ at δ = 1.81 ppm; CH_2CH_2N at δ = 1.72 ppm], is observed for **3**, indicative of metal-bound TMEDA ligands. This evidence points to the molecular structure within the crystal (vide infra) being retained in solution. Strong support for this viewpoint was gained from a variable temperature study in [D$_8$]toluene solution. At room temperature two broad resonances are observed for the $(CH_3)_2CH$ and $(CH_3)_2CH$ hydrogen atoms at δ = 3.43 and 1.31 ppm, respectively. However, on cooling the solution to −30 °C, the former resonance separates into two distinct ones at δ = 3.77 and 3.38 ppm in a 1:2 integration ratio. These resonances can be confidently assigned to terminal and bridging DA groups, respectively, and thus it can be concluded that these groups undergo a rapid dynamic equilibration at room temperature in the manner of that seen in classic dimeric structures such as $[(\mathrm{AlMe_3})_2]$.[16] The ^{1}H (and ^{13}C) NMR spectra of the potassium analogue **2** show enough similarity to those of **3** to suggest that it too retains its crystalline molecular structure in arene solution. Thus in deutero-toluene solution the $(\mathrm{CH_3})_2\mathrm{C}H$ and $(\mathrm{C}H_3)_2\mathrm{CH}$ resonances of **2** shift by only 0.03 and 0.02 ppm respectively (to lower frequency) than those in **3** and the corresponding ^{13}C resonances differ by only 0.6 and 0.2 ppm (shifted to higher and lower frequency respectively) than those in **3**. A slight anomaly seemingly exists when considering the ^{1}H resonances associated with TMEDA: the order of the $\mathrm{C}H_2$ and $Me_2\mathrm{N}$ resonances (at $\delta = 1.91$ and 1.89 ppm respectively) is reversed compared to that for **3** (corresponding values $\delta = 1.76$ and 1.84 ppm). However, the limited chemical shift range of all the signals involved (covering a mere 0.15 ppm), and, more importantly, the substantial margin between these and those of free TMEDA (i.e., $\mathrm{C}H_2$, $\delta = 2.32$ ppm; $Me_2\mathrm{N}$ $\delta = 2.11$ ppm) would appear to refute any notion that the TMEDA is not attached to the K^+ centre in **2**.

Figure 1 shows the asymmetric unit of the crystal structure of **1**, while Figure 2 captures a view of a section of the infinite, one-dimensional arrangement. Its primary feature is the familiar tris-amido motif, here consisting of a $[\mathrm{K}(\mu\text{-N})_2\mathrm{Mg}]$ ring (strictly planar) with an additional amide N "terminus" on the Mg centre. Connected by the N terminus on one interacting with the K centre of the other, two such tris-amido motifs make up the asymmetric units, which interconnect through similar K−N linkages to generate an infinite spiral chain. All the intermolecular tris-amido connection points are reinforced by agostic K···C interactions. Table 1 records the principal bond lengths and bond angles for **1**. A noteworthy observation is the lack of distinction in the Mg−N bond lengths. The notional terminal ones (Mg1−N3; Mg2−N6) display a mean length (2.046 Å) longer, not shorter, than that of the bridging type (2.037 Å), but by a mere 0.009 Å. This reflects the fact that the former DA ligands are not actually terminal but bridging (through intermolecular contacts between tris-amido units). A similar lack of distinction is found for the K−N bond lengths (mean: intramolecular bridges, 2.9351 Å; intermolecular bridges, 2.9297 Å). Thus with the intramolecular and intermolecular bridging having approximately equal weighting, the bonding can therefore be best described as genuinely supramolecular (polymeric) in nature, as opposed to that of a single tris-amido molecule with weak extended forces. An army of short, agostic K···C contacts involving both methyne and methyl groups helps to strengthen the K-$(\mu\text{-N})_2$-Mg-N framework. Disorder in two of the *i*Pr branches (those labelled C16/17/18 and C34/35/36) precludes discussion of bond lengths involving them, though they almost certainly make as important a contribution as those now mentioned. For both K atoms, the shortest of these contacts involve intramolecularly bound methyne groups [K1···C8, 3.126(2) Å; K2···C23, 3.135(3) Å]. The closest such intermolecular contacts are again to methyne C atoms [K1···C32, 3.420(2) Å; K2···C14, 3.288(2) Å]. Other K···C contacts range from 3.138(2)−3.516(3) Å for K1 and 3.167(2)−3.506(3) Å for K2. Though hydrogen atoms were not independently refined in this study, it can be assumed from the short K···C contact distances that the K atoms also lie in close proximity to $\mathrm{C}H_3$ and/or $\mathrm{C}H$ hydrogen atoms. This may have some bearing on the propensity of **1** to undergo β-hydride elimination.[10] Turning to bond angles, the Mg atoms display distorted trigonal planar geometries. To make the bridge within the $[\mathrm{K}(\mu\text{-N})_2\mathrm{Mg}]$ ring, the endocyclic N−Mg−N bond angle must compress (mean value, 112.78°). A concomitant widening occurs at the exocyclic N−Mg−N positions (mean value, 123.58°), but not symmetrically as one bond angle (mean, 125.72°) is significantly more obtuse than the other (mean, 121.43°). The coordination geometry of the K centres is less well-defined in keeping with its softer, Lewis acidic character (compared to that of Mg). With respect to N atoms, the K atoms are trigonal pyramidal (sum of bond angles: 352.64° for K1; 356.08° for K2) with two obtuse (mean, 141.87°) and one acute (mean, 70.61° belonging to the $[\mathrm{K}(\mu\text{-N})_2\mathrm{Mg}]$ ring) N−K−N bond angles, but including the close K···C contacts the coordination number of the alkali metal could be considered as high as twelve.

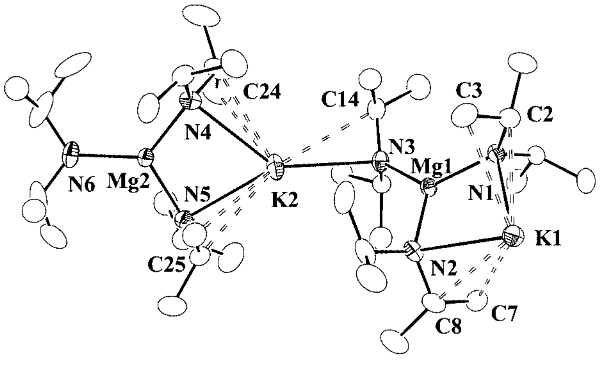

Figure 1. Asymmetric unit of the molecular structure of **1** with agostic contacts shown as broken lines; hydrogen atoms are omitted for clarity

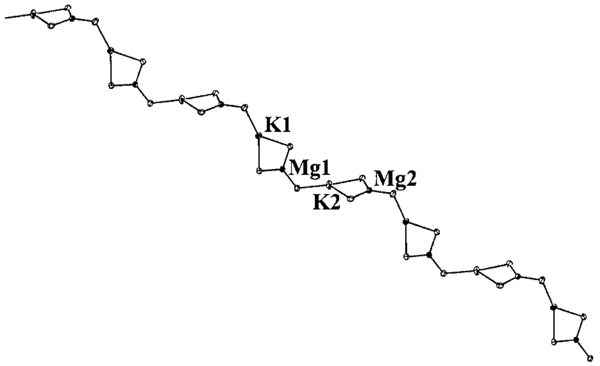

Figure 2. A section of the extended structure of **1**

Table 1. Selected bond lengths (Å) and bond angles (°) for $[\{KMg(N\textit{i}Pr_2)_3\}_\infty]$ (**1**)

Bond lengths (Å)		Bond angles (°)	
K(1)−N(6)′	2.9379(18)	N(2)−K(1)−N(6)′	136.80(5)
K(1)−N(1)	2.9595(17)	N(2)−K(1)−N(1)	70.53(5)
K(1)−N(2)	2.9181(17)	N(6)′−K(1)−N(1)	145.31(5)
K(1)···C(2)	3.138(2)	N(3)−K(2)−N(5)	146.08(5)
K(1)···C(3)	3.270(2)	N(3)−K(2)−N(4)	139.31(5)
K(1)···C(8)	3.126(2)	N(5)−K(2)−N(4)	70.69(5)
K(1)···C(7)	3.285(2)	N(1)−Mg(1)−N(2)	112.83(7)
Mg(1)−N(1)	2.0301(17)	N(1)−Mg(1)−N(3)	125.04(7)
Mg(1)−N(2)	2.0435(18)	N(2)−Mg(1)−N(3)	122.10(7)
Mg(1)−N(3)	2.0524(18)	N(5)−Mg(2)−N(4)	112.74(8)
K(2)−N(3)	2.9215(17)	N(5)−Mg(2)−N(6)	120.77(8)
K(2)−N(4)	2.9332(19)	N(4)−Mg(2)−N(6)	126.41(8)
K(2)−N(5)	2.9215(17)	Mg(1)−N(1)−K(1)	87.87(6)
K(1)···C(24)	3.167(2)	Mg(1)−N(2)−K(1)	88.76(6)
K(1)···C(14)	3.288(2)	Mg(2)−N(4)−K(2)	88.18(6)
K(1)···C(15)	3.506(3)	Mg(1)−N(5)−K(2)	88.39(6)
K(1)···C(25)	3.301(3)		
Mg(2)−N(4)	2.0395(18)		
Mg(2)−N(5)	2.0340(19)		
Mg(2)−N(6)	2.0396(19)		

The tris-amido motif also dominates the structure of **2** though now it is contained within a discrete molecular arrangement (Figure 3). This modification is due to the introduction of the didentate, chelating TMEDA ligand. By completing a distorted tetrahedral coordination sphere around K^+, the TMEDA ligation kills the need for any intermolecular K−N interactions. Table 2 records the principal bond lengths and bond angles for **2**. The distorted trigonal planar Mg coordination sphere is marked by long Mg-(μ-N) (mean length, 2.0418 Å) and short terminal Mg−N bonds [length, 1.9722(13) Å], in line with coordination number differences (i.e., 3 for N1; 4 for N2/N3). Only the latter bond shows a significant shortening compared to those in **1**, reflecting its genuine terminal nature. Adding to the asymmetry of the essentially planar $[K(\mu\text{-}N)_2Mg]$ trapezoidal ring, there is one long and one short K-(μ-N) bond (difference in length, 0.054 Å). These bonds clearly represent the weak points of the tris-amido motif given that their Mg-(μ-N) counterparts are on average 0.848 Å shorter. A comparison with the series of potassium hexamethyldisilazide $[(Me_3Si)_2N^-$; HMDS] complexes $[\{K(ar)_2\}^+\{Mg(HMDS)_3\}^-]$[17] (ar = benzene, toluene or *para*-xylene) shows that it is possible to completely cleave the large alkali metal from its tris-amido magnesiate partner (severing all K−N linkages, but retaining agostic K···C connections) by introducing π-binding arene ligands. It is significant that the K atoms in **2** ignored the toluene solvent molecules generated in the reaction by protonation of benzylpotassium. This is because TMEDA fulfils the donor responsibility in **2**, and effectively at that going on the lengths of the dative K−N bonds (mean, 2.8759 Å) which, unusually, are of the same magnitude (mean, 2.8899 Å) as their anion-containing K-(μ-N) comrades. In the aforementioned homometallic relative $[(KDA\cdot TMEDA)_2]$,[12] the K−N "anionic" bonds are significantly shorter than their dative counterparts (mean values, 2.771 and 2.886 Å respectively). Worthy of comment is the marked variation between the length of the shortest K−N (from DA) bond in this homodimer [2.706(2) Å] and that of the corresponding shortest bond in heterodimeric **2** [K−N2, 2.8630(13) Å]: this emphasises the profound proximal effect that the introduction of a Mg atom can exert on the dimensions of an identical K coordinative environment (here involving four N atoms, two from DA and two from TMEDA). The presence of TMEDA in **2** also lessens the need for reinforcement K···C agostic bonding. This is manifested in fewer K···C contacts and much longer contact distances than those previously discussed for **1**. There are only three such contacts below 4 Å in length: the shortest is to the methyl C17 at 3.277 Å, the next shortest is to the methyne C10 at 3.303 Å, and the remaining contact is to the methyl C11 at 3.475 Å. There are no intermolecular K···C contacts present, in keeping with the monomeric (dinuclear) constitution of the structure.

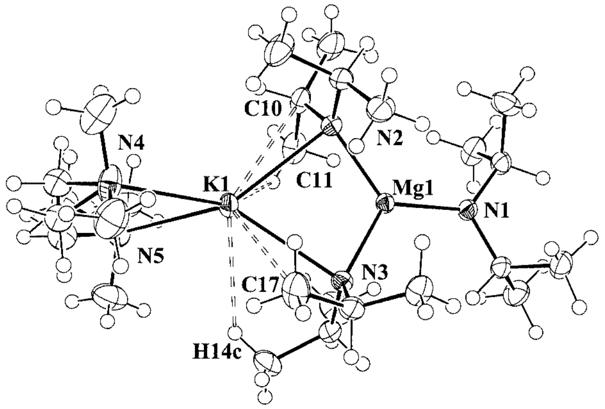

Figure 3. Molecular structure of **2** with agostic contacts shown as broken lines

Table 2. Selected bond lengths (Å) and bond angles (°) for $[KMg(N\textit{i}Pr_2)_3(TMEDA)]$ (**2**)

Bond lengths (Å)		Bond angles (°)	
Mg(1)−N(1)	1.9722(13)	N(4)−K(1)−N(2)	131.82(4)
Mg(1)−N(2)	2.0381(13)	N(2)−K(1)−N(5)	132.33(4)
Mg(1)−N(3)	2.0454(13)	N(4)−K(1)−N(3)	139.84(4)
K(1)−N(2)	2.8630(13)	N(2)−K(1)−N(3)	72.60(3)
K(1)−N(3)	2.9169(13)	N(5)−K(1)−N(3)	126.64(4)
K(1)−N(4)	2.8413(15)	N(1)−Mg(1)−N(2)	126.56(6)
K(1)−N(5)	2.9105(14)	N(1)−Mg(1)−N(3)	119.51(6)
K(1)···C(10)	3.303(2)	N(2)−Mg(1)−N(3)	113.87(6)
K(1)···C(11)	3.475(2)	Mg(1)−N(2)−K(1)	86.96(4)
K(1)···C(17)	3.303(2)	Mg(1)−N(3)−K(1)	131.82(4)

Since the metal-N core of the molecular structure of the sodium congener **3** (Figure 4) is essentially isostructural to that of **2**, it merits only a brief discussion. Table 3 records the principal bond lengths and bond angles for **3**. There is a marginally greater deviation in the bridging and terminal Mg−N (from DA) bond lengths [2.0613 Å (mean) and

1.9679(13) Å, respectively] than that in **2**. Comparison with the dimensions of the homodimeric structure of $[(NaDA\cdot TMEDA)_2]$,[11] where the mean Na−N (from DA) bond length is 2.447 Å, reveals again the strong bonding power of the proximate Mg atom in **3** as it draws the amido N bridges away from the Na atom to elongate the Na−N bonds (mean length, 2.5313 Å). To compensate the Na atom in **3** for this loss in valency, there is a concomitant strengthening of the dative bonding to TMEDA as reflected by short Na−N bonds (mean length, 2.5504 Å; *cf.* 2.6195 Å in the homodimer). Within the Na-(μ-N)$_2$-Mg trapezoidal ring, the obtuse bond angle is at Mg [110.44(5)°] and the acute one is at the larger Na centre [83.94(4)°], with a mean angle at N of 82.72°. Switching to the yet larger K centre in **2**, as expected, exacerbates this trapezoidal distortion to give corresponding values of 113.87(6)°, 72.60(3)°, and 86.17° respectively. Finally it should be noted that there are no Na···C agostic interactions in **3**, with the shortest such contact being 3.239 Å.

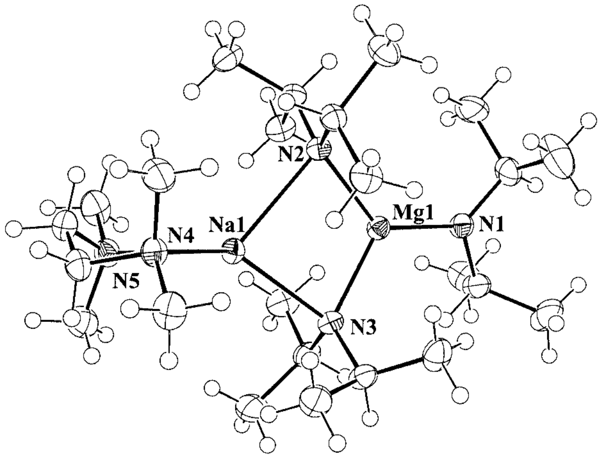

Figure 4. Molecular structure of **3**

Table 3. Selected bond lengths (Å) and bond angles (°) for $[NaMg(NiPr_2)_3(TMEDA)]$ (**3**)

Bond lengths (Å)		Bond angles (°)	
Mg(1)−N(1)	1.9679(13)	N(2)−Na(1)−N(5)	126.82(5)
Mg(1)−N(2)	2.0638(13)	N(2)−Na(1)−N(4)	134.30(5)
Mg(1)−N(3)	2.0587(13)	N(2)−Na(1)−N(3)	83.94(4)
Na(1)−N(2)	2.4988(13)	N(5)−Na(1)−N(3)	125.29(4)
Na(1)−N(3)	2.5638(13)	N(4)−Na(1)−N(3)	116.98(4)
Na(1)−N(4)	2.5537(13)	N(1)−Mg(1)−N(3)	131.34(6)
Na(1)−N(5)	2.5472(14)	N(1)−Mg(1)−N(2)	118.00(5)
		N(3)−Mg(1)−N(2)	110.44(5)
		Mg(1)−N(3)−Na(1)	81.95(4)
		Mg(1)−N(2)−Na(1)	83.49(4)

Structural differences in the solid state, if maintained in solution, can influence the reaction chemistry of the DA anion given the close correlation that exists between structure and reactivity. A brief survey of a selection of previously determined *s*-block metal-based DA structures (see Figure 5) is therefore warranted to enable the novelty of the structures of **1**−**3** to be put into perspective. Pure crystalline LDA exists as a helical polymer (**A**) with near linear NLiN segments, eight of which constitute a turn of the helix.[18] More relevant to the solution phase, the solvated derivative $[(LDA\cdot THF)_2]$ (**B**) exhibits a planar (LiN)$_2$ dimeric ring, the Li corners of which carry monodentate THF ligands.[19] A similar discrete four-membered ring structure (**B**) is observed in both the aforementioned $[(NaDA\cdot TMEDA)_2]$[11] and $[(KDA\cdot TMEDA)_2]$,[12] though the wider exocyclic coordination arcs offered by the larger alkali metals allows for the chelation of didentate TMEDA ligands. Combining LDA with the same diamine molecule in $[\{(LDA\cdot TMEDA)_2\}_\infty]$[20] again generates a (LiN)$_2$ dimeric ring, but the reduced space about the Li centres forces the TMEDA ligands into bridging (non-chelating) roles to create an infinite chain of linked dimers (**C**). It may be significant from a reactivity standpoint that the exclusively bridging mode of the DA ligands in all of the last four structures discussed contrasts with the combination of bridging and terminal modes encountered in both **2** and **3** (and possibly in **1** depending on its fragmentation process in solution). The opportunity for **1**−**3** to dissociate in the form of a complex "ate" anion $[Mg(DA)_3]^-$, which is unavailable to the homometallic compositions, may also cause them to react differently towards protic substrates. To the best of our knowledge, this tris-DA coordination about Mg is unique to the structures of **1**−**3** though it is known with other metals both discretely, for example with A1 in neutral monomeric $[A1(DA)_3]$ (**D**),[21] or linked into the common dimeric motif as with Mn in $[\{Mn(DA)_2\}_2]$ (**E**).[22] On the other hand bis-DA coordination of Mg is well-known when auxiliary ligands are present to fill the remaining sites: it is only rarely observed in homomagnesium structures such as the mixed alkynyl/DA dimer $[\{Mg(DA)(C{\equiv}CPh)\cdot THF\}_2]$ (**E**),[23] where the linearity of the alkynyl ligand allows for a tetrahedral Mg coordination, but is much more common in heterometallic examples, and these can exhibit three (trigonal planar), or more usually, four (tetrahedral) Mg coordination depending on the steric characteristics of the ligand sets, as illustrated by the alkide $[Me_2A1(DA)_2MgMe]$ (**G**)[24] and the amidinate $[Me_2A1(DA)_2Mg\{tBuNC(Me)NtBu\}]$ (**H**)[25] respectively. While mixed aluminium-magnesium complexes of this type are commonplace, in general, the range of heterometallic magnesium-containing DA-based crystal structures is rather limited. Extending the search to other related amide ligands reveals a far higher number of hits of "ate" complexes with the general formula $[Mg(amide)_3]^-$. HMDS complexes of this type are particularly commonplace as exemplified by the aforementioned π-arene series $[\{K(ar)_2\}^+ \{Mg(HMDS)_3\}^-]$.[17] The recent report of the trimetallic lithium-potassium-(bis)magnesium N-metallated/N,C-dimetallated amide $[Li_2K_2Mg_4\{tBu(Me_3Si)N\}_4\{tBu[Me_2(H_2C)Si]N\}_4]$,[26] an inverse crown molecule with an atomless cavity, suggests there is every possibility that the rich structural variety found within the s-block chemistry of the DA ligand is far from exhausted.

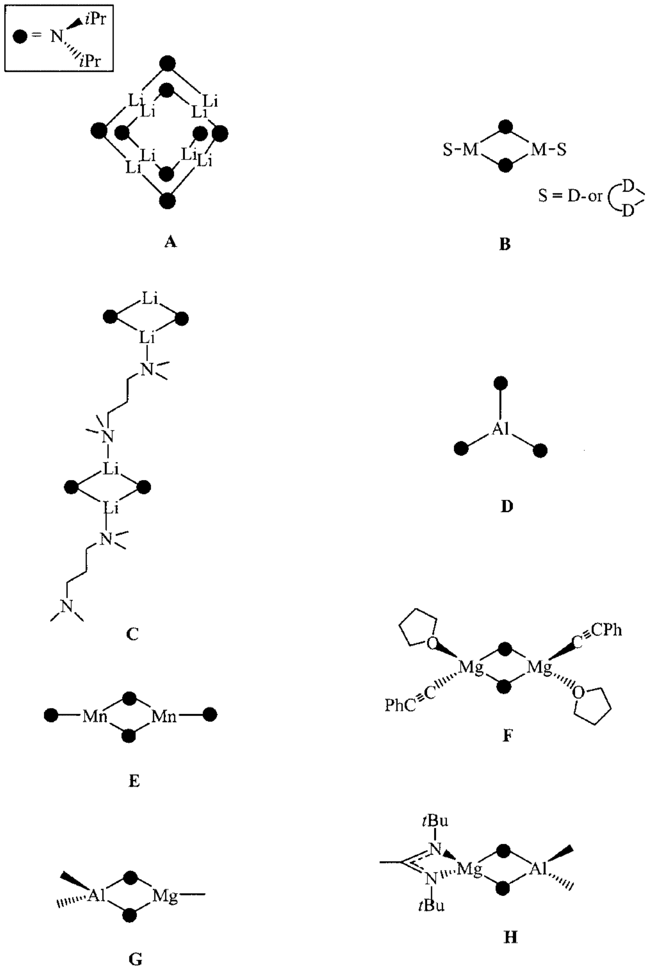

Figure 5. Selected structures in the *s*-block chemistry of the DA ligand and related structures

Experimental Section

General: All reactions were performed under a protective argon atmosphere using standard Schlenk techniques. Hexane was dried by heating to reflux over sodium benzophenone ketyl and distilled under nitrogen prior to use. Diisopropylamine was dried by heating to reflux over calcium hydride and stored over 4 Å molecular sieves. *n,s*-Dibutylmagnesium was purchased from Aldrich Chemicals as a 1 M solution in heptane and standardised immediately prior to use using salicylaldehyde phenylhydrazone.[27] Benzylpotassium,[28] butylpotassium[29] and butylsodium[30] were prepared according to the literature methods. Melting points were determined in sealed argon-filled capillary tubes and are uncorrected. NMR experiments were carried out on a Bruker DPX 400 MHz spectrometer, operating at 400.13 MHz for ^{1}H and 100.62 MHz for ^{13}C.

[{KMg(DA)$_3$}$_\infty$] (1): (From butylpotassium) A 1:1:3 stoichiometric mixture of *n*BuK (0.4 g, 5 mmol)/*n,s*-Bu$_2$Mg (5 mL of a 1 M solution in heptane, 5 mmol)/*i*Pr$_2$NH (2.1 mL, 15 mmol) in hexane (15 mL) was stirred at ambient temperature overnight. This resulted in the formation of a brown oily solution with a trace amount of a black waxy solid. The solid was removed by filtering the mixture through Celite. The filtrate was reduced in volume in vacuo, then placed in the freezer at −28 °C. Overnight this solution deposited a crop of colourless crystals of **1** (yield 0.49 g, 27%). M.p. 96−98 °C (decomposes to brown oil). Satisfactory microanalyses could not be obtained due to samples losing weight rapidly on the balance.^{1}H NMR ([D$_6$]benzene solution; 25 °C): δ = 3.38 (sep., 1 H, Me$_2$C*H*), 1.27 (d, 6 H, *Me*$_2$CH).
(From benzylpotassium) Benzylpotassium (0.65 g, 5 mmol) was suspended in hexane (20 mL). *n,s*-Bu$_2$Mg (5 mL of a 1 M solution in heptane, 5 mmol) and *i*Pr$_2$NH (2.1 mL, 15 mmol) were then added. The reaction mixture was stirred for 12 hours at ambient temperature. The resulting cloudy red mixture was filtered through Celite and the filtrate was concentrated by removing some solvent in vacuo. Freezer cooling of the solution at −28 °C afforded a crop of colourless crystals of **1** (yield 0.62 g, 34%). Characterisation as above but in addition: ^{1}H NMR ([D$_8$]toluene solution; 25 °C): δ = 3.30 (sep., 1 H, Me$_2$C*H*), 1.21 (d, 6 H, *Me*$_2$CH) ppm. ^{13}C NMR ([D$_8$]toluene solution; 25 °C): δ = 49.7 (Me$_2$*C*H), 27.92 (*Me*$_2$CH) ppm.

[KMg(DA)$_3$·TMEDA] (2): Benzylpotassium (0.65 g, 5 mmol) was suspended in hexane (20 mL). *n,s*-Bu$_2$Mg (5 mL of a 1 M solution in heptane, 5 mmol) and *i*Pr$_2$NH (2.1 mL, 15 mmol) were then introduced. The resulting red solution was stirred for 30 minutes after which time TMEDA (0.75 mL, 5 mmol) was added. After stirring for a further 60 minutes, the solution was concentrated by removing some solvent in vacuo. Freezer cooling of the remaining solution at −28 °C produced a crop of colourless crystals of **2**. These were partially covered by a red oil which hindered the isolation of the pure crystalline material and precluded a meaningful determination of its yield. Satisfactory microanalyses could not be obtained due to contamination by the red oily coating. ^{1}H NMR ([D$_8$]toluene solution; 25 °C): δ = 3.40 [m (broad), 6 H, Me$_2$C*H*], 1.91 (s, 4 H, C*H*$_2$, TMEDA), 1.89 (s, 12 H, C*H*$_3$, TMEDA), 1.29 [d (broad), 36 H, *Me*$_2$CH] ppm. ^{13}C NMR ([D$_8$]toluene solution; 25 °C): δ = 57.2 (*C*H$_2$, TMEDA), 49.8 (Me$_2$*C*H), 45.4 (*C*H$_3$, TMEDA), 27.9 (*Me*$_2$CH) ppm.

[NaMg(DA)$_3$·TMEDA] (3): *n*BuNa (0.4 g, 5 mmol) was suspended in hexane (10 mL) and placed in an ultrasonic bath for 10 minutes. *n,s*-Bu$_2$Mg (5 mL of a 1 M solution in heptane, 5 mmol) was introduced slowly to give a brown gum, which dissolved upon the addition of *i*Pr$_2$NH (2.1 mL, 15 mmol). The resulting pale yellow solution was stirred for 20 minutes at which time TMEDA (0.75 mL, 5 mmol) was added. Turning cloudier, the solution was stirred for a further 20 minutes, filtered through Celite, reduced in volume in vacuo, and left to cool in the freezer at −28 °C. After several days a crop of colourless crystals of **3** was obtained (isolated yield 0.51 g, 22% − the bulk of the crystalline product redissolved during the isolation procedure). M.p. 103−105 °C. Satisfactory microanalyses (C,H,N) were obtained. ^{1}H NMR ([D$_6$]benzene solution; 25 °C): δ = 3.50 (sep., 6 H, Me$_2$C*H*), 1.81 (s, 12 H, C*H*$_3$, TMEDA), 1.72 (s, 4 H, C*H*$_2$, TMEDA), 1.38 (d, 36 H, *Me*$_2$CH) ppm. ^{1}H NMR ([D$_8$]toluene solution; 25 °C): δ = 3.43 [m (broad), 6 H, Me$_2$C*H*], 1.84 (s, 12 H, C*H*$_3$,TMEDA), 1.76 (s, 4 H, C*H*$_2$, TMEDA), 1.31 [d (broad), 36 H, *Me*$_2$CH] ppm. ^{1}H NMR ([D$_8$]toluene solution; −30 °C): δ = 3.77 [s (broad), 2 H, Me$_2$C*H*], 3.38 [s (broad), 4 H, Me$_2$C*H*, μ-DA] 1.75 [s, 12 H, C*H*$_3$, TMEDA], 1.60 [d, 4 H, C*H*$_2$, TMEDA], 1.27[s (broad), 36 H, *Me*$_2$CH] ppm. ^{13}C NMR ([D$_8$]toluene solution; 25 °C): δ = 57.4 (*C*H$_2$, TMEDA), 49.2 (Me$_2$*C*H), 46.2 (*C*H$_3$, TMEDA), 28.1 (*Me*$_2$CH) ppm.

X-ray Structure Determinations: Measurements were made on a Nonius Kappa CCD diffractometer at 123 K with Mo-K_α radiation (λ = 0.71073 Å). Structures were refined on F^2 using all reflections with the Shelxl-97 program. All non-H atoms were treated anisotropically except for the disordered components in **1** and **2**. H atoms were not refined except for those involved in agostic interactions in **2**. Further crystallographic data and refinement parameters are given in Table 4. CCDC-213563 (**1**), -213564 (**2**) and -213565 (**3**) contain the supplementary crystallographic data for this paper. These data can be obtained free of charge at www.ccdc.cam.ac.uk/conts/retrieving.html [or from the Cambridge Crystallographic Data Centre, 12, Union Road, Cambridge CB2 1EZ, UK; Fax: (internat.) +44-1223/336-033; E-mail: deposit@ccdc.cam.ac.uk].

Table 4. Crystallographic data for compounds **1−3**

	1	**2**	**3**
Empirical formula	$C_{18}H_{42}KMgN_3$	$C_{24}H_{58}KMgN_5$	$C_{24}H_{58}MgN_5Na$
Molecular weight	363.96	480.16	464.05
Crystal system	triclinic	monoclinic	orthorhombic
Space group	$P\bar{1}$	$P2_1/n$	Pbca
a (Å)	9.9818 (1)	10.1715 (1)	18.2113 (5)
b (Å)	14.3537 (2)	20.5215 (3)	16.9186 (4)
c (Å)	15.8388 (3)	15.4082 (2)	20.0492 (6)
α (°)	92.479 (1)	90	90
β (°)	91.747 (1)	101.598 (1)	90
γ (°)	90.414 (1)	90	90
V (Å^3)	2266.06 (6)	3150.55 (7)	6177.4 (3)
Z	4	4	8
2θ max.	27.64	27.87	26.79
No. of reflections	10414	7500	6554
No. of parameters	430	295	296
$R1$	0.0516	0.0453	0.0438
$wR2$	0.1273	0.1046	0.1045
S	1.031	1.025	1.057

Acknowledgments

We thank the UK EPSRC for funding this research through grant award number GR/R81183/01.

---

[1] For reviews of the uses of lithium amides in synthesis see: J. K. Crandall, M. Apparu, *Org. React.* **1983**, *29*, 345−443; V. Snieckus, *Chem. Rev.* **1990**, *90*, 879−933; C. H. Heathcock, in *Comprehensive Organic Synthesis* (Eds: B. M. Trost, I. Fleming), Pergamon, New York, **1991**, vol. 2, chapter 1.6; T. Satoh, *Chem. Rev.* **1996**, *96*, 3303−3326.

[2] Collum has made a colossal contribution to correlating the complicated structural chemistry of LDA in solution to its performances and kinetics in organic reactions. For leading papers see: Y.-J. Kim, M. P. Bernstein, A. S. Galiano Roth, F. E. Romesberg, P. G. Williard, D. J. Fuller, A. T. Harrison, D. B. Collum, *J. Am. Chem. Soc.* **1991**, *56*, 4435−4439; J. F. Remenar, B. L. Lucht, D. B. Collum, *J. Am. Chem. Soc.* **1997**, *119*, 5567−5571; X. Sun, D. B. Collum, *J. Am. Chem. Soc.* **2000**, *122*, 2459−2463; J. L. Rutherford, D. B. Collum, *J. Am. Chem. Soc.* **2001**, *123*, 199−202.

[3] For an excellent general monologue on the multivariate factors which determine the course of an organoalkali metal-mediated reaction see: M. Schlosser, in *Organometallics in Synthesis A Manual*, 2nd Edn (Ed.: M. Schlosser), John Wiley and Sons Ltd, Chichester, England, **2002**, chapter 1, 1−352.

[4] R. E. Mulvey, *Chem. Commun.* **2001**, 1049−1056.

[5] K. J. Drewette, K. W. Henderson, A. R. Kennedy, R. E. Mulvey, C. T. O'Hara, R. B. Rowlings, *Chem. Commun.* **2002**, 1176−1177.

[6] D. J. Gallagher, K. W. Henderson, A. R. Kennedy, C. T. O'Hara, R. E. Mulvey, R. B. Rowlings, *Chem. Commun.* **2002**, 376−377.

[7] W. Clegg, K. W. Henderson, A. R. Kennedy, R. E. Mulvey, C. T. O'Hara, R. B. Rowlings, D. M. Tooke, *Angew. Chem.* **2001**, *113*, 4020−4023; *Angew. Chem. Int. Ed.* **2001**, *40*, 3902−3905.

[8] A. M. Drummond, L. T. Gibson, A. R. Kennedy, R. E. Mulvey, C. T. O'Hara, R. B. Rowlings, T. Weightman, *Angew. Chem.* **2002**, *114*, 2488−2490; *Angew. Chem. Int. Ed.* **2002**, *41*, 2382−2384.

[9] R. Sanchez, W. Scott, *Tetrahedron Lett.* **1988**, *29*, 139−142.

[10] P. Andrikopoulos, D. R. Armstrong, A. R. Kennedy, R. E. Mulvey, C. T. O'Hara, R. B. Rowlings, *following paper in this issue.*

[11] P. C. Andrews, N. D. R. Barnett, R. E. Mulvey, W. Clegg, P. A. O'Neil, D. Barr, L. Cowton, A. J. Dawson, B. J. Wakefield, *J. Organomet. Chem.* **1996**, *518*, 85−95.

[12] W. Clegg, S. Kleditzsch, R. E. Mulvey, P. O'Shaughnessy, *J. Organomet. Chem.* **1998**, *558*, 193−196.

[13] M. Micha-Screttas, C. G. Screttas, B. R. Steele, G. A. Heropoulos, *Tetrahedron Lett.* **2002**, *43*, 4871−4873.

[14] G. W. Gokel, L. Barbour, S. L. DeWall, E. S. Meadows, *Coord. Chem. Rev.* **2001**, *222*, 127−154.

[15] E. S. Meadows, S. L. DeWall, L. J. Barbour, G. W. Gokel, *J. Am. Chem. Soc.* **2001**, *123*, 3092−3107.

[16] Ch. Elschenbroich, A. Salzer, in *Organometallics A Concise Introduction*, 1st Edn, VCH, Weinheim, **1989**, pp 80−81.

[17] G. C. Forbes, A. R. Kennedy, R. E. Mulvey, B. A. Roberts, R. B. Rowlings, *Organometallics* **2002**, *21*, 5115−5121.

[18] N. D. R. Barnett, R. E. Mulvey, W. Clegg, P. A. O'Neil, *J. Am. Chem. Soc.* **1991**, *113*, 8187−8188.

[19] P. G. Williard, J. M. Salvino, *J. Org. Chem.* **1993**, *58*, 1−3.

[20] M. P. Bernstein, F. E. Romesberg, D. J. Fuller, A. T. Harrison, D. B. Collum, Q.-Y. Liu, P. G. Williard, *J. Am. Chem. Soc.* **1992**, *114*, 5100−5110.

[21] P. J. Brothers, R. J. Wehmschulte, M. M. Olmstead, K. Ruhlandt-Senge, S. R. Parkin, P. P. Power, *Organometallics* **1994**, *13*, 2792−2799.

[22] A. Belforte, F. Calderazzo, U. Englert, J. Strahle, K. Wurst, *J. Chem. Soc., Dalton Trans.* **1991**, 2419−2427.

[23] K.-C. Yang, C.-C. Chang, J.-Y. Huang, C.-C. Lin, G.-H. Lee, Y. Wang, M.-Y. Chiang, *J. Organomet. Chem.* **2002**, *648*, 176−187.

[24] T.-Y. Her, C.-C. Chang, L.-K. Liu, *Inorg. Chem.* **1992**, *31*, 2291−2294.

[25] M.-D. Li, C.-C. Chang, Y. Wang, G.-H. Lee, *Organometallics* **1996**, *15*, 2571−2574.

[26] G. C. Forbes, F. R. Kenley, A. R. Kennedy, R. E. Mulvey, C. T. O'Hara, J. A. Parkinson, *Chem. Commun.* **2003**, 1140−1141.

[27] B. E. Love, E. G. Jones, *J. Org. Chem.* **1999**, *64*, 3755−3756.

[28] D. Hoffmann, W. Bauer, F. Hampel, N. J. R. van Eikema Hommes, P. v. R. Schleyer, P. Otto, U. Pieper, D. Stalke, D. S. Wright, R. Snaith, *J. Am. Chem. Soc.* **1994**, *116*, 528−536.

[29] R. Pi, W. Bauer, B. Brix, C. Schade, P. v. R. Schleyer, *J. Organomet. Chem.* **1986**, *306*, C1−C4.

[30] C. Schade, W. Bauer, P. v. R. Schleyer, *J. Organomet. Chem.* **1985**, *295*, C25−C28.

Received June 27, 2003